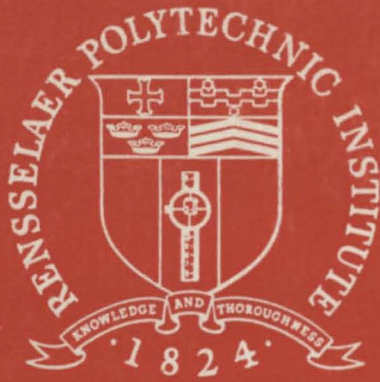


RP1-TR-PT-6804



PROJECT TUBEFLIGHT

W. D. ERNST

RECIRCULATORY FLOW IN A CYLINDRICAL CAVITY

TR PT 6804

RECIRCULATORY FLOW
IN A
CYLINDRICAL CAVITY

by
William D. Ernst

This work was supported in part by the National Science Foundation under Grant No. NSF-GK-618 and constitutes part of a thesis to be submitted to the faculty of the School of Engineering in partial fulfillment of the requirements for the degree of Doctor of Philosophy.

RENSSELAER POLYTECHNIC INSTITUTE
TROY, NEW YORK

September 1968

ACKNOWLEDGMENT

The author wishes to express his appreciation and gratitude to Dr. H. J. Hagerup for suggesting the problem and providing advice and guidance throughout the work.

SUMMARY

An investigation is made of the laminar, large Reynolds number, two-dimensional recirculatory flow induced in a circular cylinder by the steady tangential motion of a segment of the periphery. A review of the pertinent published literature indicates that the theoretical and experimental results are inconclusive, except for the observation that the flow field configuration may be idealized as a constant-vorticity core surrounded by a boundary layer along the wall. With the assumption of this flow configuration, a solution for the peripheral boundary layer is derived by utilizing for the stationary and the moving wall respectively two linearized forms of the laminar boundary layer equation, each containing an arbitrary stretching-function. The mathematical solution to the problem is approached through a Fredholm integral equation for the boundary layer velocity distribution. For the primitive case where the two stretching-functions for simplicity are assumed to be equal to the same constant, results are calculated which are in complete agreement with previous work by Mills. A second paper is being prepared in which the correct stretching-functions are actually determined for the present problem.

TABLE OF CONTENTS

	Page
SUMMARY	i
LIST OF SYMBOLS	iii
INTRODUCTION	1
General	1
Historical Background	2
PROBLEM FORMULATION	7
Basic Model	7
Governing Equations	8
Derivation of General Solution	12
A Qualitative Solution	20
CONCLUDING DISCUSSION	24
APPENDIX I	26
APPENDIX II	30
APPENDIX III	32
REFERENCES	35
FIGURES	37

LIST OF SYMBOLS

- a length of moving segment of S_b in physical plane
 \hat{a} length of moving segment of S_b in \hat{x}_m plane
 b breadth of cavity
 c length of stationary segment of S_b in physical plane
 \hat{c} length of stationary segment of S_b in \hat{x}_s plane
 d depth of cavity
 F force on S_b
 $k(x)$ von Mises stretching function
 k_0 constant approximating von Mises stretching function
 K $K = U_c/U$ core velocity ratio
 $\lambda(x)$ Oseen stretching function
 λ_0 constant approximating Oseen stretching function
 R_c $R_c = Ub/\nu$, Reynolds number based on cavity breadth
 R_e $R_e = U_c \lambda b/\nu$ Reynolds number based on flow length
 S_b outermost closed streamline of recirculation flow field
 u velocity parallel to wall
 U constant velocity of moving segment of S_b
 U_c constant velocity at outer edge of core
 U_∞ free stream velocity of external flow field in cavity flow
 v $v = \hat{u}_s^2 - K^2$
 w $w = \hat{u}_m^2 - K^2$
 x distance measured parallel to wall in physical plane
 \hat{x} $\hat{x} = \int_0^x 1/k(\rho) d\rho$ distance parallel to wall in transformed plane

y distance measured normal to wall

ρ density

ν kinematic viscosity

λ $\lambda = c/a$ wall length ratio

ψ $\psi = \int u dy$ stream function

Subscripts

m refers to moving wall

s refers to stationary wall

INTRODUCTION

GENERAL

Laminar recirculatory flow fields are common in aerodynamics, and occur for example behind bluff bodies, in discontinuous expansions, ahead of forward facing steps, and in cavities. In addition, the flow fields associated with peripheral jet and plenum chamber vehicle support devices in translation are of a recirculatory nature. The present study is concerned with a laminar version of a particular type of recirculatory flow field encountered in the context of plenum chamber support devices.

The steady state recirculatory flow field to be considered is subject to the following restrictions: First, the location of the "bounding-streamline" of the recirculatory flow field, S_b , will be considered fixed and independent of both the external and the internal, recirculatory flow fields. Second, the velocity along the bounding-streamline will be assumed piecewise constant. Third, the recirculatory flow field will be assumed amenable to division into an inner constant-vorticity core centered in the flow field with a constant velocity U_c at its periphery, and a thin boundary layer located adjacent to S_b with a velocity distribution periodic in arc length.

The problem of determining the velocity distribution in this boundary layer represents a special case of the classical "continuation problem" formulated by Prandtl¹ in 1904. The periodic solution¹ corresponding to recirculatory flow is of obvious importance to the full understanding of the general continuation problem, and should be relatively less difficult to verify through experimental observation. An experimental program is in fact being undertaken in parallel with the present theoretical investigation, and will be reported elsewhere.

HISTORICAL BACKGROUND

Recirculatory flow fields in general are divided into two types depending on the nature of the bounding-streamline S_b . The first, or "free-streamline", type is the more common and also the more difficult to analyze. In this problem the location of the bounding-streamline S_b is at least in part not known a priori, and must be determined by matching the internal and external pressure and velocity distributions. The second, or "fixed-streamline" type strictly speaking includes only those recirculatory flows completely surrounded by solid boundaries of fixed location. However, many flow fields not altogether surrounded by fixed boundaries still have the location of S_b so closely suggested by the physical circumstances that they may be analyzed as if S_b were known and fixed. In addition, many free-streamline recirculatory flow problems are amenable to iterative methods of solution, where the location of S_b is initially assumed, the internal and external flow subsequently calculated as in a fixed-streamline problem, and the inconsistency gradually removed by a succession of improved assumptions of S_b .

Two of the parameters commonly used to describe these flow fields are the wall length ratio, $\lambda = c/a$, where c and a are the lengths of the stationary and moving segments of S_b , respectively, and the core velocity fraction $K = U_c/U$, where U is the velocity of the moving segment of S_b . In the free-streamline case, U is not known a priori and depends on the interaction of the internal and external flow. However, in a previous work on recirculatory flow, Mills² suggests that U be approximated by 55 percent of the free stream velocity of the external flow field. This value will be used herein as the definition of U for all cavity flow fields in order to facilitate the comparison of free-streamline and fixed-streamline

results.

Problems relating to the "free-streamline" type of recirculatory flow have been solved for a number of special cases. Using potential theory, Ringleb³ derived the general inviscid velocity distribution along the wall for a class of cusp cavities, under the assumption that a standing vortex forms within the cavity. Thom and Apelt⁴ calculated the flow in certain two-dimensional rectangular cavities at low Reynolds numbers using a finite difference technique. Batchelor⁵ derived the condition that the vorticity is uniform within the core of a closed flow for sufficiently large Reynolds numbers. Using this condition, Wood⁶ determined, from an exact analysis, the core velocity fraction K as a function of the velocity distribution along S_b . For the recirculatory flow considered herein, his analysis yields the result that $K = 1/\sqrt{1+\lambda}$.

Roshko⁷ measured the pressure and velocity distributions in a rectangular cavity on the floor of a wind tunnel for two free stream velocities, $U_\infty = 75$ fps and 200 fps. This cavity had a fixed breadth b and an adjustable depth d . He obtained a series of profiles showing boundary layer behavior near S_b , but only in one case did his velocity traverse extend far enough into the interior of the cavity to sense the presence of the inviscid core. This traverse was made parallel to the bottom of the cavity at a depth $d/2$, and indicated the presence of a thin boundary layer on the walls, and the outer portion of what appears to be the core region. The boundary layer had a characteristic Reynolds Number $Re = \frac{\lambda b U_c}{\nu} \approx 10^5$ and was probably laminar. At the upstream side, the core velocity ratio was found to be $K = 0.49$, while at the downstream edge, $K = 0.71$. The flow pattern is thus not symmetric, and the pressure distribution along S_b would not be expected to be constant. Pressure measurements along the walls of the cavity

indicate a large increase in pressure towards the downstream cavity wall. As the d/b ratio of the cavity was changed continuously, it was also observed that the flow in the cavity was bi-stable for $1.2 < d/b < 1.8$. The particular pressure measured at the downstream edge of the cavity was dependent upon whether this range of d/b was entered from above or below. This suggests the formation of a second core region inside the cavity.

Because of its relative simplicity there exists a larger body of work on the "fixed-streamline" case. Weiss and Florsheim⁸ published an analysis of the fixed-streamline rectangular cavity flow valid for streaming motion. Their results indicate that for $d/b = 1$, there is a single core, nearly symmetric in the streamwise direction, and centered at $y/b = .78$, where y is the distance measured from the bottom of the cavity. For $d/b = 2$, a second but substantially weaker core is formed.

In addition, Weiss and Florsheim made visual studies at low Reynolds numbers of an analogous free-streamline flow and obtained results which agreed qualitatively with their theoretical results. They observed the onset of formation of a second core for $d/b = 1.7$, which is approximately the upper limit of Roshko's⁷ bi-stable regime. This suggests that if the effect responsible for Roshko's bi-stable regime is indeed the formation of a second core, then the occurrence of a second core depends on d/b alone and not on Reynolds number.

Mills⁹, Burggraf¹⁰, and Pan and Acrivos¹¹ attacked the low Reynolds number ($R_c < 400$) case of a fixed-streamline flow field, and obtained numerical solutions of the full Navier-Stokes equations for a rectangular cavity of varying d/b ratios. They also verified their solutions qualitatively by flow visualization experiments. Their iterative method of solution is rapidly convergent at low Reynolds number but cannot conveniently

be extended to a Reynolds number much larger than 400.

Squire¹² treated the fixed streamline large Reynolds number case for a cylindrical cavity having half its periphery in motion ($\lambda = 1$). Squire's method of solution was to assume the existence of an inviscid core and a surrounding boundary layer, and then to linearize the boundary layer equation by using the Oseen approximation, replacing $u \frac{\partial u}{\partial x} + v \frac{\partial u}{\partial y}$ by $k_0 u \frac{\partial u}{\partial x}$ in the boundary layer equation. (The product $k_0 u$ is sometimes denoted as a "convection velocity", but, since the implications of this term are incorrect, k_0 will be called the Oseen constant herein). Next, as a working assumption, he assumes the value 0.5 for the core velocity ratio K , and he also chooses that value for the Oseen constant k_0 . Squire's analysis for $\lambda = 1$ yields the result that $K = 0.5$. Squire argues that his velocity at the edge of the core has been correctly taken to be $0.5U$, because the solution obtained on that basis gives zero torque applied by the walls to the fluid in the cylinder. However, Squire's method of solution cannot be very accurate because the best choice for the Oseen constant is certainly not the same for a stationary wall as for a wall moving in the flow direction.

Another analysis of the peripheral viscous problem is contained in a second paper by Mills,² who considered the flow in a square cavity with one wall moving ($\lambda = 3$). He assumes a core-boundary layer model as does Squire, but unlike Squire he chooses to use the von Mises form of the boundary layer equations,

$$\frac{1}{u} \frac{\partial u^2}{\partial x} = \nu \frac{\partial^2 u^2}{\partial y^2}$$

This expression is then linearized by replacing $1/u$, the coefficient of $\frac{\partial u^2}{\partial x}$ by k_0/U where k_0 is denoted herein as the von Mises constant.

Following a suggestion by Wood⁶ he chooses k_0 to be the reciprocal of the rms of the velocity along S_b , i.e. $k_0 = 2$. Using these assumptions, he determines that $K = 0.5$ and argues that this value is correct since the net torque in the cavity is zero. As already mentioned, Mills made experimental measurements of recirculatory flow fields of both the free and fixed streamline type. His velocity profiles for both cases show a nearly symmetric centered inviscid core surrounded by a thin boundary layer. For the free streamline case at $R_c \approx 10^5$, Mills considers his flow to be turbulent and shrinks his y -scale by the amount necessary to make his velocity profile data agree with the theory. Alternatively, since the velocity profiles depend strongly on the value of the von Mises constant, as in Squire's analysis, this effect may be an indication that an incorrect value was used for k_0 . The observed values of K were .5 and .15 for the free and fixed streamline cases respectively, although he suggests the latter result may be erroneous due to experimental difficulties.

Before proceeding with the analysis, the following observations can be made in summary. Recirculatory flow fields with a constant-vorticity core surrounded by a boundary layer are obtained in the laboratory for sufficiently high Reynolds number. For recirculatory flow fields having $d/b \approx 1$, the core is nearly centered in the flow field, and the flow configuration appears to be unique.

PROBLEM FORMULATION

BASIC MODEL

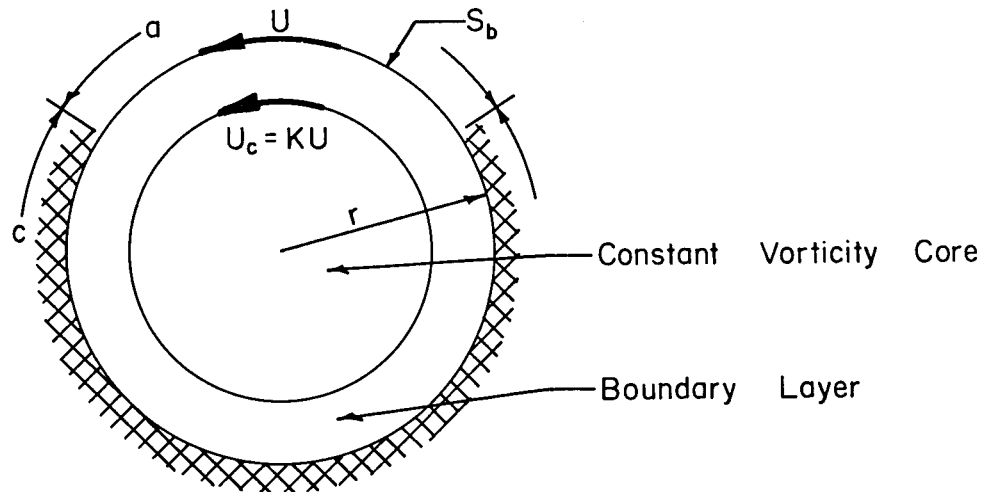


Fig. 1.

The steady two-dimensional fixed-streamline flow field considered is contained within an infinite circular cylinder of radius γ . A segment of the periphery, of length a , consists of a solid wall moving tangentially at the velocity U , and the remainder of the periphery, of length c , consists of a solid stationary wall. If the Reynolds number is large enough, the flow pattern will be characterized by a thin boundary layer along the walls and a central rotating core. In the analysis to follow, it will be assumed that the core is concentric to the cylinder, has constant vorticity, and has a tangential velocity of KU at its edge. Correspondingly, it will be assumed that the boundary layer, because of its thinness, is the same as that on a flat wall in a free stream of constant velocity KU and the boundary conditions at the wall of zero slip velocity and constant slip velocity U for segments of length c and a , respectively. Two constraints are imposed which are not normally part of boundary layer theory, but which are obvious from the original circular flow version of the problem. First, since under the assumption of steady

recirculatory flow any fluid particle must return to its initial position with the same velocity it had when it started, the boundary layer must be periodic of period $(a + c)$. Second, since under the same assumption of steady flow there is zero net torque on the core, the integral of the shear stress taken along the entire periphery must be zero.

GOVERNING EQUATIONS

The two-dimensional laminar incompressible boundary layer equation for a flow with constant freestream velocity, when combined with the continuity equation, yields:

$$u \frac{\partial u}{\partial x} - \frac{\partial u}{\partial y} \int_0^y \frac{\partial u}{\partial x} dy = \nu \frac{\partial^2 u}{\partial y^2} \quad (1a)$$

The boundary layer equation is, of course, nonlinear, and even for the simple case of uniform flow past a solid surface, the only exact solutions are determined from lengthy numerical iteration or series expansion procedures. In the present case, where the initial velocity distribution is an unknown function of y to be determined implicitly from the analysis, an approach in terms of the full boundary layer equations seem overly ambitious, and various methods of obtaining an approximate solution were explored. Of the methods examined, an approach to the problem through linearization of the boundary layer equations appeared most promising in terms of its simplicity and flexibility. Two different approaches, each yielding the same form for the linearized boundary layer equation, are considered in detail below.

The classical approximation due to Oseen replaces the left hand side of equation 1a by $U \frac{\partial u}{\partial x}$, where U is the freestream velocity. This linearization procedure works very well where the local velocity differs from the free stream velocity by a small amount, as for instance, in the

problem of wake development far downstream. However, for the Prandtl boundary layer problem this method of solution gives a value of the shear stress which is high by 76 percent. Lewis and Carrier¹¹ suggested that this linearization procedure be modified by replacing the left hand side of equation 1a by $l_0 U \frac{\partial u}{\partial x}$ where the constant l_0 represents some appropriate average of the normalized velocity in the vicinity of the wall, i.e. $0 < l_0 < 1$. For simple flow problems having constant initial and boundary conditions this modified linearization procedure should be adequate. However, for more complicated problems an improved linearization method is required, since a constant l_0 would not indicate the decreasing dependence with increasing distance of the wall shear stress on the initial velocity distribution. One such improved approach is to replace the left hand side of equation 1a by $l U \frac{\partial u}{\partial x}$, where $l = l(x)$, $l(y)$ or $l(x,y)$ is denoted as the Oseen stretching function for reasons made obvious later. This approach was used, among other authors, by Sparrow and Lin¹⁴ in an analysis of the entrance effect in tubes.

There are many methods by which l may be determined depending on the particular problem but each of these requires at least two criteria. First, since an approximate solution can at best correctly represent only a small portion of the true flow field, a decision must be made as to which property of the flow the approximate solution should represent with the least error. A few of the properties that could be used are values at a point in space such as boundary layer thickness or momentum thickness, or on a surface in space such as inertia or shear stress. Second, a criterion must be established regarding which additional constraint on the problem will be used to determine l , so that it best represents the desired property. For flow situations in which an exact solution is known, the obvious

constraint is that the approximate solution for the desired property equal the exact solution for the desired property. For instance, if one considers the flat plate boundary layer problem and requires that the ℓ -dependent approximate solution for the shear stress at the wall be correct, then one discovers that $\ell(x) = \ell_0 = 0.346$. For the present problem, there is of course no exact solution available, and ℓ must be determined a priori. In order to formulate the problem it is presently sufficient to assume the existence of the function ℓ . Its determination will be deferred to a second paper.

If it is assumed that $\ell = \ell(x)$, this Oseen stretching function approach yields that the governing equation for the boundary layer flow equivalent to equation 1a is

$$\ell(x) u \frac{\partial u}{\partial x} = \nu \frac{\partial^2 u}{\partial y^2} \quad (1b)$$

As an alternative to improving the method used by Oseen, one can choose to linearize the von Mises¹⁵ form of the boundary layer equations,

$$\frac{1}{u} \frac{\partial u^2}{\partial x} = \nu \frac{\partial^2 u^2}{\partial \psi^2} \quad (2a)$$

which is equivalent to equation 1a. This form is the result of introducing the coordinate transformation $y = \int \frac{d\psi}{u}$, where ψ is the stream function. If the left hand of equation 2a is replaced by $\frac{k(x)}{u} \frac{\partial u^2}{\partial x}$ where k is denoted as the von Mises stretching function, then we obtain a second linearized equation equivalent to equation 1a, namely

$$\frac{k(x)}{u} \frac{\partial u^2}{\partial x} = \nu \frac{\partial^2 u^2}{\partial \psi^2} \quad (2b)$$

This equation is linear in u and has the same form as equation 1b.

However, the use of equation 2b instead of equation 1b for the present

analysis appears to have two advantages. First equation 2b describes the forces on a fluid particle in the "natural" coordinate system (x, ψ) . Second, the von Mises equation has been successfully used by Wood in an exact analysis which appears to predict K correctly for the present problem. A similar analysis by Squire, using the Oseen equation instead is apparently incorrect since it predicts a value of K which disagrees with Woods' result. For these reasons the analysis to follow will be based on equation 2a alone.

The present analysis will be undertaken in terms of the two undefined von Mises stretching functions, i.e., $k_m(x)$ for the moving wall and $k_s(x)$ for the stationary wall. The reasons behind the choice of a different k for the moving wall and the stationary wall will be considered in a later section.

By redefining the variables in the following manner

$$\begin{aligned} x^* &= x/a & \psi^* &= \psi / (aU R^{-1/2}) \\ u^* &= u/U & R &= aU/\nu \end{aligned} \quad (3)$$

equation 2a is made dimensionless and of the following form

$$k(x) \frac{\partial u^{*2}}{\partial x^*} = \frac{\partial^2 u^{*2}}{\partial \psi^{*2}} \quad (4)$$

Henceforth, all of the analysis will be performed using dimensionless variables and, for simplicity, the asterisk will be dropped. Equation 4 may be simplified further by absorbing $k(x)$ in a coordinate stretching transformation of the form

$$\frac{\partial}{\partial \bar{x}} = k(x) \frac{\partial}{\partial x} \quad (5a)$$

The linearized boundary layer equation then takes the form

$$\frac{\partial \hat{u}^2}{\partial \hat{x}} = \frac{\partial^2 \hat{u}^2}{\partial \psi^2} \quad \text{where} \quad \hat{u}(\hat{x}, \psi) = u(x, y) \quad (5b)$$

At the end of the analysis, the physical x coordinate is reintroduced through the expression

$$x = \int_0^{\hat{x}} k(\rho) d\rho \quad (5c)$$

Equations 5 with an initial condition and two boundary conditions comprise the mathematical formulation of the linearized problem.

DERIVATION OF GENERAL SOLUTION

In order to provide for different $k(x)$ on the moving and stationary walls, the recirculatory flow field is determined from the solution of two separate but interdependent subproblems: the development along a stationary wall of a boundary layer with an arbitrary initial velocity distribution, and the same problem but with respect to a moving wall. It is permissible to divide the problem this way since the linearized boundary layer equation is parabolic; thus the downstream boundary conditions do not affect the upstream flow field. The solutions of the two subproblems are interdependent because the velocity distribution at the end of the stationary wall constitutes the initial velocity distribution on the moving wall, and the velocity distribution at the end of the moving wall constitutes the initial velocity distribution on the stationary wall.

A typical example of the velocity distributions on the moving and stationary walls in the transformed x coordinate system is sketched in Fig. 3. It is important to note that the length of wall in the \hat{x} coordinate system (denoted by \hat{a} and \hat{c} for the moving and stationary wall, respectively) is as yet undetermined and will depend on the function $k(x)$.

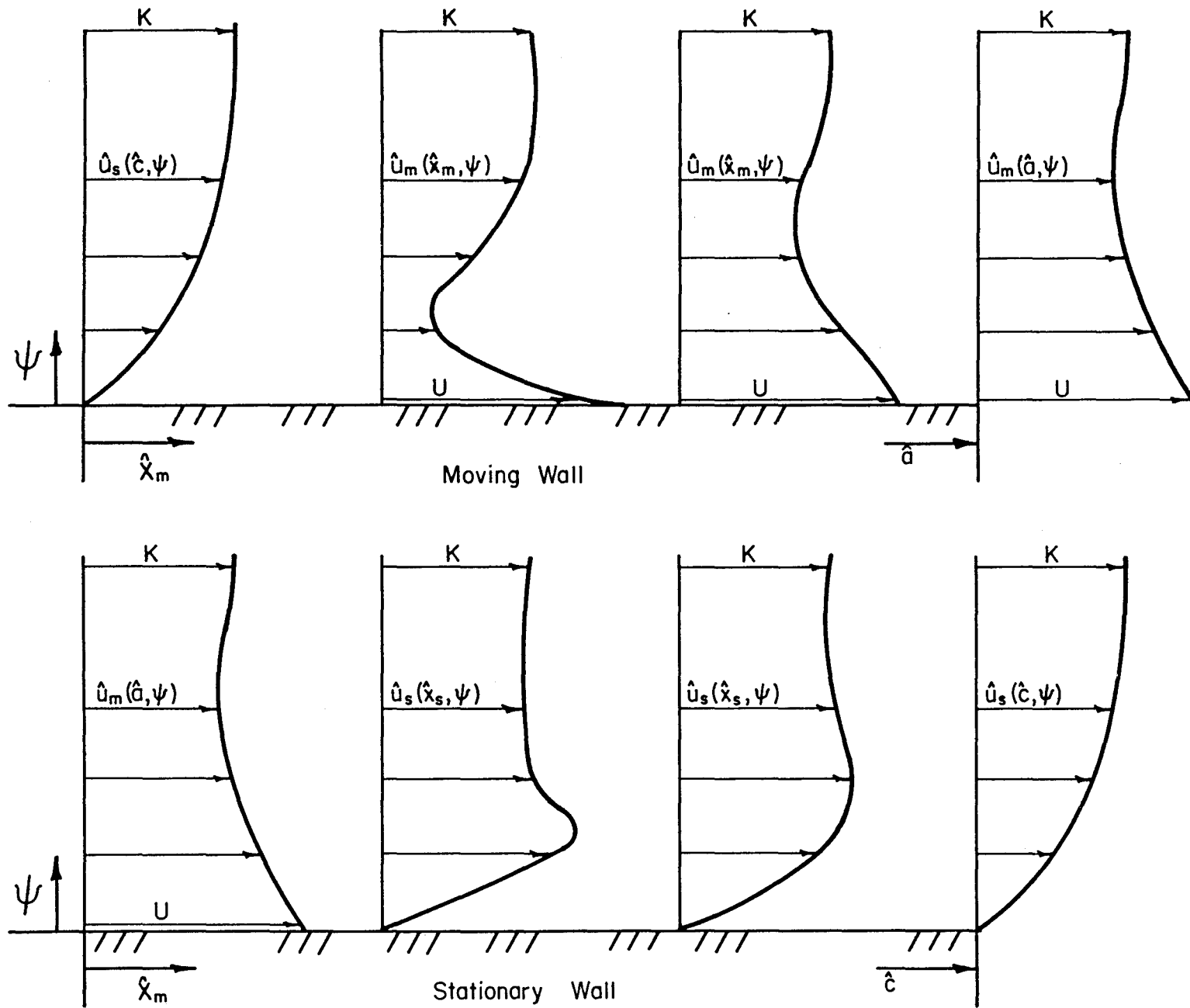


Fig. 2. Typical Boundary Layer Development

The problem of determining the recirculatory flow field is thus reduced to the simultaneous solution of the following two boundary value problems:

$$\begin{aligned}
 \text{a) } \quad & \frac{\partial \hat{u}_s^2}{\partial \hat{x}_s} = \frac{\partial^2 \hat{u}_s^2}{\partial \psi^2} && \begin{cases} 0 < \hat{x}_s < \hat{c} \\ 0 < \psi < \infty \end{cases} \\
 & \hat{u}_s^2(0, \psi) = \hat{u}_m^2(\hat{a}, \psi) \\
 & \hat{u}_s^2(\hat{x}_s, 0) = 0 \\
 & \lim_{\psi \rightarrow \infty} \hat{u}_s^2(\hat{x}_s, \psi) = K^2
 \end{aligned} \tag{6a}$$

$$\begin{aligned}
 \text{b) } \quad & \frac{\partial \hat{u}_m^2}{\partial \hat{x}_m} = \frac{\partial^2 \hat{u}_m^2}{\partial \psi^2} && \begin{cases} 0 < \hat{x}_m < \hat{a} \\ 0 < \psi < \infty \end{cases} \\
 & \hat{u}_m^2(0, \psi) = \hat{u}_s^2(\hat{c}, \psi) \\
 & \hat{u}_m^2(\hat{x}_m, 0) = 1 \\
 & \lim_{\psi \rightarrow \infty} \hat{u}_m^2(\hat{x}_m, \psi) = K^2
 \end{aligned} \tag{6b}$$

In order to make the boundary conditions at infinity homogeneous, and simultaneously simplify the analysis, let us make the change of variables

$$\begin{aligned}
 w &= \hat{u}_m^2 - K^2 \\
 v &= \hat{u}_s^2 - K^2
 \end{aligned}$$

which reduces the problem to the following form

$$\begin{aligned}
 \frac{\partial v}{\partial \hat{x}_s} &= \frac{\partial^2 v}{\partial \psi^2} && \begin{cases} 0 < \hat{x}_s < \hat{c} \\ 0 < \psi < \infty \end{cases} \\
 v(0, \psi) &= w(\hat{a}, \psi) \\
 v(\hat{x}_s, 0) &= -K^2 \\
 \lim_{\psi \rightarrow \infty} v(\hat{x}_s, \psi) &= 0
 \end{aligned} \tag{7a}$$

$$\frac{\partial w}{\partial x_m} = \frac{\partial^2 w}{\partial \psi^2} \quad \begin{cases} 0 < \hat{x}_m < \hat{a} \\ 0 < \psi < \infty \end{cases}$$

$$w(0, \psi) = v(\hat{c}, \psi)$$

$$w(x_m, 0) = 1 - k^2$$

$$\lim_{\psi \rightarrow \infty} w(\hat{x}_m, \psi) = 0$$
(7b)

The initial-boundary value problems of equations 7a, 7b are first transformed to end point problems in the s-plane by means of the Laplace transform

$$\bar{w}(s, \psi) = \int_0^{\infty} e^{-s\hat{x}} w(\hat{x}, \psi) d\hat{x}$$

with the result

$$\bar{v}_{\psi\psi} - s\bar{v} = -w(\hat{a}, \psi)$$

$$\bar{v}(s, 0) = -k^2/s$$

$$\lim_{\psi \rightarrow \infty} \bar{v}(s, \psi) = 0$$
(8a)

$$\bar{w}_{\psi\psi} - s\bar{w} = -v(\hat{c}, \psi)$$

$$\bar{w}(s, 0) = (1 - k^2)/s$$

$$\lim_{\psi \rightarrow \infty} \bar{w}(s, \psi) = 0$$
(8b)

The solution of equations 8a, 8b may now be determined for an arbitrary initial velocity profile. Since the equations for the stationary wall and the moving wall are of an identical form, only the solution procedure for the former will be presented in detail.

The Green's function for the solution of equation 8a is determined from the associated homogeneous problem

$$g_{yy} - s g = 0$$

$$g(s, 0) = 0$$

$$\lim_{\psi \rightarrow \infty} g(s, \psi) = 0$$
(9)

Thus, the Green's function for equation 8a is the solution of

$$\begin{aligned} g_{yy} - s y &= \delta(y-\xi) \\ g(s,0) &= 0 \\ \lim_{y \rightarrow \infty} g(s,y) &= 0 \end{aligned} \quad (10)$$

It is easily seen that this problem yields as a result

$$g(y, \xi, s) = \begin{cases} -\frac{1}{2\sqrt{s}} \left[e^{-\sqrt{s}(y+\xi)} - e^{-\sqrt{s}(\xi-y)} \right], & y < \xi \\ -\frac{1}{2\sqrt{s}} \left[e^{-\sqrt{s}(y+\xi)} - e^{-\sqrt{s}(y-\xi)} \right], & y > \xi \end{cases} \quad (11)$$

and thus the solution of equation 8a with homogeneous boundary conditions is

$$\bar{v} = \int_0^{\infty} g(y, \xi, s) \bar{w}(\hat{a}, \xi) d\xi \quad (12)$$

To determine the solution with nonhomogeneous boundary conditions, we assume

$$\bar{v} = \int_0^{\infty} g(y, \xi, s) \bar{w}(\hat{a}, \xi) d\xi + P(y) \quad (13)$$

The function P must satisfy the following equation and boundary conditions

$$\begin{aligned} P_{yy} - sP &= 0 \\ P(0) &= -k^2/s \\ \lim_{y \rightarrow \infty} P(y) &= 0 \end{aligned} \quad (14)$$

and is found to be

$$P(y) = -k^2/s e^{-\sqrt{s}y} \quad (15)$$

It follows then that the solutions of Equations 5a, 5b in the s-plane can be given in the form

$$\bar{v}(s, \psi) = \int_0^{\infty} g(\psi, \xi, s) w(\hat{a}, \xi) d\xi - k^2/s e^{-\sqrt{s} \psi} \quad (16a)$$

$$\bar{w}(s, \psi) = \int_0^{\infty} g(\psi, \xi, s) v(\hat{c}, \xi) d\xi + (1-k^2)/s e^{-\sqrt{s} \psi} \quad (16b)$$

Formally transforming back to the s-plane, we obtain the velocity distributions

$$v(\hat{x}_s, \psi) = \int_0^{\infty} g_1(\psi, \xi, \hat{x}_s) w(\hat{a}, \xi) d\xi - k^2 \operatorname{erfc}\left(\sqrt{\frac{1}{\hat{x}_s}} \frac{\psi}{2}\right) \quad (17a)$$

$$w(\hat{x}_m, \psi) = \int_0^{\infty} g_1(\psi, \xi, \hat{x}_m) v(\hat{c}, \xi) d\xi + (1-k^2) \operatorname{erfc}\left(\sqrt{\frac{1}{\hat{x}_m}} \frac{\psi}{2}\right) \quad (17b)$$

where

$$g_1(\psi, \xi, \hat{x}) = \frac{1}{2\sqrt{\pi \hat{x}}} \left[\exp\left(\frac{-(\psi-\xi)^2}{4\hat{x}}\right) - \exp\left(\frac{-(\psi+\xi)^2}{4\hat{x}}\right) \right] \quad (18)$$

It may easily be shown that the formal results given by equations 17a, 17b are the valid solutions of equations 7a, 7b. Noting that

$$v(\hat{c}, \xi) = v(\hat{x}_s, \xi) \Big|_{\hat{x}_s = \hat{c}} \quad \text{one may combine equations 17a,}$$

17b to give a single equation for $w(\hat{a}, \psi)$

$$w(\hat{a}, \psi) = \int_0^{\infty} g_1(\psi, \xi, \hat{a}) \left\{ \int_0^{\infty} g_1(\xi, \xi', \hat{c}) w(\hat{a}, \xi') d\xi' - k^2 \operatorname{erfc}\left(\sqrt{\frac{1}{\hat{c}}} \frac{\psi}{2}\right) \right\} d\xi + (1-k^2) \operatorname{erfc}\left(\sqrt{\frac{1}{\hat{a}}} \frac{\psi}{2}\right) \quad (19)$$

The solution of this equation is the velocity distribution at the end of the moving wall. Equation 19 is a singular Fredholm integral equation of the second kind with an iterated kernel, solvable in terms of a Neumann's series.¹⁶ The obvious compactness of equation 19 is the reason an integral equation approach was taken to the simultaneous solution of equations 7a and 7b.

Briefly, Neumann's series may be obtained in the following manner. An initial approximation for the velocity profile $w(\hat{a}, \psi)$ is obtained from the nonhomogeneous part of the integral equation, and is substituted as $w(\hat{a}, \xi')$ in the inner integral on the right hand side of equation 19. The result of performing the indicated operations is an improved $w(\hat{a}, \xi)$ which can then be used in the same manner for a second calculation. The procedure is repeated until the desired accuracy is obtained. Symbolically, the solution of equation 19 may be given by

$$\overset{(m)}{w}(\hat{a}, \psi) = G(\hat{a}, \psi) + \overset{(m)}{I} \overset{(m-1)}{w}(\hat{a}, \psi), \quad m \geq 1 \quad (20)$$

where m indicates the order of the approximation, $G(\hat{a}, \psi) = (1-k) \operatorname{erfc}(\sqrt{\frac{1}{\alpha}} \frac{\psi}{2})$ and I, J are operators such that

$$\begin{aligned} \overset{(n)}{I} &= \overset{(n-1)}{I} \overset{(n-2)}{I} \dots \overset{(2)}{I} \overset{(1)}{I} \\ I f(x) &= \int_0^x J(x, \xi) f(\xi) d\xi \end{aligned} \quad (21a)$$

and

$$\begin{aligned} J(x, \xi) f(\xi) &= g_1(\psi, \xi, \hat{a}) \int_0^\infty g_2(\psi, \xi, \hat{c}) f(\xi) d\xi \\ &\quad - k^2 \operatorname{erfc}(\sqrt{\frac{1}{\alpha}} \frac{\psi}{2}) \end{aligned} \quad (21b)$$

It can be shown that the solution is independent of the initial approximation for $w(\hat{a}, \psi)$. Also, as shown in Appendix I, the solution is valid for all \hat{a}, \hat{c} and $\psi \in 0 < \psi < \infty$.

The algebra of the operations required in equation 20 is routine except for the evaluation of integrals of the form

$$\int_0^\infty \frac{1}{2\sqrt{\pi\alpha}} \operatorname{erf}(\sqrt{\frac{1}{\alpha}} \frac{\psi}{2}) \left\{ \exp\left(\frac{-(\psi-\xi)^2}{4\alpha}\right) - \exp\left(\frac{-(\psi+\xi)^2}{4\alpha}\right) \right\} d\xi \quad (22)$$

This integral, as shown in Appendix II, may be evaluated to give

$$\operatorname{erf}\left(\sqrt{\frac{1}{\alpha+\gamma}} \frac{\psi}{2}\right) \quad (23)$$

Making repeated use of this result, and taking $\hat{w}^{(0)} = 0$, Neumann's method yields

$$\begin{aligned} \hat{w}^{(1)}(\hat{a}, \psi) &= (1-k^2) - \mathcal{O}(\hat{a}) + k^2 \mathcal{O}(\hat{z}) \\ \hat{w}^{(p)}(\hat{a}, \psi) &= (1-k^2) - \mathcal{O}(\hat{a}) + k^2 \mathcal{O}(\hat{z}) \\ &\quad + \sum_{n=2}^p \left\{ (1-k^2) \mathcal{O}((n-1)\hat{z}) - \mathcal{O}((n-1)\hat{z} + \hat{a}) \right\} \\ &\quad + k^2 \mathcal{O}(p\hat{z}), \quad p > 1 \end{aligned} \quad (24)$$

where

$$\mathcal{O}(\eta) = \operatorname{erf}\left(\sqrt{\frac{1}{\eta}} \frac{\psi}{z}\right)$$

and

$$\hat{z} = \hat{a} + \hat{c}$$

Since as shown in Appendix I this series converges uniformly, it may be regrouped to give

$$\hat{w}^{(p)}(\hat{a}, \psi) = \sum_{n=1}^p \left\{ \mathcal{O}((n-1)\hat{z}) - \mathcal{O}((n-1)\hat{z} + \hat{a}) \right\} + (1-k^2) + k^2 \mathcal{O}(p\hat{z}) \quad (25)$$

$$\text{With } \hat{u}_m^2 = w + k^2, \quad \hat{u}_s^2 = v + k^2$$

equation 25 may be substituted into equation 17a to yield

$$\begin{aligned} \hat{u}_s^2(\hat{x}_s, \psi) &= \sum_{n=1}^p \left\{ \mathcal{O}((n-1)\hat{z} + \hat{x}_s) - \mathcal{O}((n-1)\hat{z} + \hat{a} + \hat{x}_s) \right\} \\ &\quad + k^2 \mathcal{O}(p\hat{z} + \hat{x}_s) \end{aligned} \quad (26)$$

Similarly, equation 26 substituted into equation 17b yields

$$\begin{aligned} \hat{u}_m^2(\hat{x}_m, \psi) &= \sum_{n=1}^p \left\{ \mathcal{O}((n-1)\hat{z} + \hat{c} + \hat{x}_m) - \mathcal{O}(n\hat{z} + \hat{x}_m) \right\} \\ &\quad + 1 - \mathcal{O}(\hat{x}_m) + k^2(p\hat{z} + \hat{c} + \hat{x}_m) \end{aligned} \quad (27)$$

It is easily verified that the solutions given by equations 26, 27 satisfy the boundary conditions, the initial conditions, and the differential equations everywhere except at the points $\hat{x}_m = y = 0$ and $\hat{x}_s = y = 0$, where there is a step discontinuity in the boundary conditions.

An investigation of the solution for small x reveals that the singularity is the same as that encountered at the leading edge in the classical flat plate problem. This singularity is integrable, so the shear stress on the moving wall may be determined without difficulty.

Although it has not yet been necessary to specify the stretching functions k_m and k_s , a transformation of our results to the physical plane requires that these functions be known. It is not within the scope of this paper to accurately determine k_m and k_s and a complete discussion of this question will be made in a subsequent paper. However, some qualitative observations bearing on k_m and k_s are made on a simple basis in the next section.

A QUALITATIVE SOLUTION

A crude method for obtaining a preliminary value of k would obviously be to determine k such that the k -dependent solution for say, shear stress at the wall, obtained from the present linearized boundary layer equation for a particular problem, agrees with an exact solution, obtained from the full boundary layer equation for the same problem. For the present, we select as the basis for this determination the two following simple, steady-state, two-dimensional, boundary layer flows with constant initial velocity profiles: the classical Blasius problem, and the moving wall problem. The first involves the flat plate boundary layer produced by a uniform flow of velocity U_c along a semi infinite stationary sharp edged flat plate aligned with the stream. The second involves the boundary layer flow produced in an initially quiescent medium by the motion at constant velocity, U of the surface of a semi-infinite stationary plate in a plane parallel to the plate. Howarth¹⁷ has determined that the shear stress at the wall in the Blasius problem is given by

$$\tau_0 = .332 \rho U_c \sqrt{\frac{2}{U_c x}}$$

while the author has determined that the shear stress at the wall in the moving wall problem is given by $\tau_0 = -0.444 \rho U^2 \sqrt{\frac{\nu}{2Ux}}$

The linearized solution for the Blasius problem yields

$$\tau_0 = \sqrt{k_{s_0}} \frac{1}{2\sqrt{\pi}} \rho U_c \sqrt{\frac{\nu}{2U_c x}}$$

and for the moving wall problem $\tau_0 = -\sqrt{k_{m_0}} \frac{1}{2\sqrt{\pi}} \rho U \sqrt{\frac{\nu}{2Ux}}$

with $k_m(x)$ and $k_s(x)$ assumed to be the constants k_{m_0} and k_{s_0} , respectively.

It is easily seen that the use of $k_{m_0} = 2.50$ and $k_{s_0} = 1.38$ in the linearized analysis for these two simple problems will yield a shear stress which agrees with the exact result. If the linearized solutions had been normalized with respect to U as is done in the remainder of this paper, the appropriate results would have been $k_{m_0} = 2.50$ and $k_{s_0} = 1.38/K$, where $K = U_c/U$.

For the case when the initial velocity is not a constant, the lack of an exact solution prevents one from determining the stretching functions by the method above. In this case, the assumption that k_m and k_s are constant along the wall would not appear to be valid because the dependency of shear stress upon the initial velocity profile decreases with increasing distance downstream. It would appear, consequently, that the correct k_m and k_s must be nonequal, nonconstant functions of x .

Despite these reservations let us assume, in the interests of simplicity, and with the expectation of a solution at least qualitatively correct, that k_m and k_s are the nonequal arbitrary constants, k_{m_0} and k_{s_0} . The transformation connecting the plane in which this problem is solved and the physical plane becomes, from equation 5c

$$\begin{aligned} \hat{x}_m &= x/k_{m_0} & \hat{x}_s &= x/k_{s_0} \\ \hat{a} &= a/k_{m_0} & \hat{c} &= c/k_{s_0} \end{aligned}$$

Hence, the solutions in the physical plane for the boundary layer velocity distributions are

$$\hat{u}_s^{(p)}(x, \psi) = \hat{u}_s^{(p)}(\hat{x}_s, \psi) \Big|_{\hat{x}_s = x/k_{s_0}} \quad (28a, b)$$

$$\hat{u}_m^{(p)}(x, \psi) = \hat{u}_m^{(p)}(\hat{x}_m, \psi) \Big|_{\hat{x}_m = x/k_{m_0}}$$

Since, for steady state conditions the net torque on the flow field must be zero, the integral of the shear stress over S_b is zero, and we may determine K from

$$F_s + F_m = 0$$

where

$$F_s = \int_0^c \left(\frac{\partial}{\partial y} \hat{u}_s^{(p)}(x, y) \right)_{y=0} dx = \frac{1}{2} \int_0^c \left(\frac{\partial}{\partial \psi} \hat{u}_s^{(p)2}(x, \psi) \right)_{\psi=0} dx \quad (29a)$$

$$F_m = \int_0^a \left(\frac{\partial}{\partial y} \hat{u}_m^{(p)}(x, y) \right)_{y=0} dx = \frac{1}{2} \int_0^a \left(\frac{\partial}{\partial \psi} \hat{u}_m^{(p)2}(x, \psi) \right)_{\psi=0} dx \quad (29b)$$

Substitution of equations 26, 27 in the above relations yields

$$F_s = k_{s_0}/\sqrt{\pi} \left[\sum_{n=1}^p \left\{ ((n-1)\bar{e} + \bar{c})^{1/2} - ((n-1)\bar{e})^{1/2} - ((n-1)\bar{e} + \bar{a} + \bar{c})^{1/2} + ((n-1)\bar{e} + \bar{a})^{1/2} \right\} + K^2 \left\{ (p\bar{e} + \bar{c})^{1/2} - (p\bar{e})^{1/2} \right\} \right] \quad (30a)$$

$$F_m = k_{m_0}/\sqrt{\pi} \left[\sum_{n=1}^p \left\{ ((n-1)\bar{e} + \bar{c} + \bar{a})^{1/2} - ((n-1)\bar{e} + \bar{c})^{1/2} - (n\bar{e} + \bar{a})^{1/2} + (n\bar{e})^{1/2} \right\} + K^2 \left\{ (p\bar{e} + \bar{c} + \bar{a})^{1/2} - (p\bar{e} + \bar{c})^{1/2} \right\} - \bar{a}^{1/2} \right] \quad (30b)$$

The determination of a K which makes $F_s + F_m = 0$ will depend only on λ and on the ratio k_{s_0}/k_{m_0} . If it is assumed at this point that exactly the same linearized equation describes the flow on the moving wall as on

the stationary wall, then the ratio k_{s_0}/k_{m_0} can be taken to be unity.

This assumption yields

$$K^{(p)2} = \frac{(p\hat{a} + p\hat{c})^{1/2} - ((p-1)\hat{a} + p\hat{c})^{1/2}}{(p\hat{a} + (p+1)\hat{c})^{1/2} - ((p-1)\hat{a} + p\hat{c})^{1/2}} \quad (31)$$

Now letting $p \rightarrow \infty$, we find

$$K^2 = \lim_{p \rightarrow \infty} K^{(p)2} = \frac{\hat{a}}{\hat{a} + \hat{c}} = \frac{1}{1 + \lambda}$$

and thus

$$K = \sqrt{1/(1 + \lambda)} \quad (32)$$

CONCLUDING DISCUSSION

The boundary layer velocity distributions given by equations 26 and 27 have been derived utilizing the single assumption that the boundary layer flow can be adequately described by the following linearized equation

$$k(x) \frac{\partial u^2}{\partial x} = \frac{\partial^2 u^2}{\partial \psi^2}$$

Whereas k_m and k_s remain to be determined in a second report, a preliminary example of the adequacy of this linearized boundary layer equation has been assessed by approximating $k_m(x)$ and $k_s(x)$ by the representative constants k_{m_0} and k_{s_0} . The solution for the boundary layer velocity distribution using these constants is given by equations 28 and 32.

The most important result indicates that the core velocity fraction K depends only on the ratio k_{s_0}/k_{m_0} , whereas the velocity distribution and the boundary layer thickness depend on the k_0 's directly. Thus Mills' use of $k_{s_0} = k_{m_0} = (\text{rms of } U)^{-1} = 2$ can have no effect on the core velocity fraction K and only influences the velocity distribution and boundary layer thickness.

A comparison of the core velocity fraction K for several investigators is shown in Figure 3. The agreement between the present solution given in equation 32 and Mills' theoretical results is to be expected, since he also used a linearized form of the von Mises equation and indirectly assumed $k_{s_0}/k_{m_0} = 1$. The present results may be considered as independent verification of Mills' solution for the simple case where $k_{s_0} = k_{m_0}$. However, Mills' results do not apply to the actual case where $k_s(x) \neq k_m(x)$ and thus are somewhat limited. The present results are also in perfect agreement with the exact solution for K given by Wood. Experimentally, Mills found that for $\lambda = 3, K \approx .15$ in a fixed-streamline flow, and $K \approx .5$ in a free-streamline flow. He attributes the large discrepancy between the experimental and theoretical results in the former case to experimental difficulties. Any comparison in the latter case can be qualitative only since theory and experiment are not for the same flow field. Likewise, Roshko's measurements in a free-streamline flow field are valid only for qualitative comparison. Basing his analysis on equation 1b with $l_{s_0} = l_{m_0} = .5$, Squire obtained the result that $K = .5$ for $\lambda = 1$, which disagrees with Wood's exact result and is thus probably wrong.

The velocity distributions within the boundary layer at four different stations, computed from equation 28 with $k_{s_0} = k_{m_0} = 2$, are plotted in Figures 4 and 5 for $\lambda = 1$ and $\lambda = 3$, respectively. These results agree with those of Mills in the $\lambda = 3$ case for the reasons cited previously. Several general observations can be made from the results presented in these figures. First, the oscillatory shear stress on the core is opposed in direction to the shear stress on the boundary layer at the wall. Second, there is a momentum flux into the core away from the stationary wall and a momentum flux out of the core towards the moving wall. It is this second

phenomenon that actually determines the motion of the core, as can be seen from a simple investigation of the start-up process.

Further discussion of the flow, and comparison of the theoretical velocity distribution results with experimental data, will be deferred to the second part of this investigation, which will introduce the non-constant, nonequal $k_s(x)$ and $k_m(x)$ provided for in the general formulation of this problem.

APPENDIX I

The derivation for the region of validity of the Neumann series solution of equation 25 is based, primarily, on the theorems of linear spaces,^{16,18} which will be quoted without proof. Equation 25 can be written simply in operator form as

$$u = \lambda C u + f \quad (\text{I-1})$$

where

$$\begin{aligned} C u &= A(B u) \\ &= \int_0^{\infty} \int_0^{\infty} g_1(\psi, \xi, \hat{a}) g_1(\xi, \xi', \hat{c}) u \, d\xi' \, d\xi \end{aligned}$$

and

$$f = k^2 \operatorname{erf}\left(\sqrt{\frac{1}{\hat{a}+\hat{c}}} \frac{\psi}{2}\right) - \operatorname{erf}\left(\sqrt{\frac{1}{\hat{a}}} \frac{\psi}{2}\right) + (1-k^2)$$

It can be shown the Equation (I-1) will possess a convergent Neumann series for any u whose norm is bounded (i.e. $\|u\| = \left\{ \int_0^{\infty} |u|^2 \, d\psi \right\}^{1/2} < \infty$) providing that $|\lambda| < 1/\|C\|$, where $\|C\|$ is the bound of the integral transformation, defined by $\|C\| = \operatorname{lub}_{\|u\| \neq 0} \frac{\|Cu\|}{\|u\|} = \|AB\|$. In order to simplify the determination of $\|C\|$, we will make use of the inequality $\|AB\| < \|A\| \|B\|$, which is demonstrated for the present kernel in Appendix III.

Now denoting

$$\begin{aligned} w(\psi) &= B u(\psi) \\ &= \int_0^{\infty} g_1(\psi, \xi, \hat{a}) u(\xi) \, d\xi \\ &= \frac{1}{2} \int_0^{\infty} (\exp(-b(\psi-\xi)^2) - \exp(-b(\psi+\xi)^2)) u(\xi) \, d\xi \end{aligned}$$

where $b = 1/4\hat{a}$, $d = 2\sqrt{\pi\hat{a}}$

we have

$$\begin{aligned} \omega^2(\psi) = \frac{1}{d^2} \int_0^\infty \int_0^\infty & \left\{ e^{-b(\psi-\xi)^2} e^{-b(\psi-t)^2} u(\xi) u(t) \right. \\ & - e^{-b(\psi-\xi)^2} e^{-b(\psi+t)^2} u(\xi) u(t) \\ & - e^{-b(\psi+\xi)^2} e^{-b(\psi-t)^2} u(\xi) u(t) \\ & \left. + e^{-b(\psi+\xi)^2} e^{-b(\psi+t)^2} u(\xi) u(t) \right\} d\xi dt \end{aligned}$$

If in each of the four integrals above we let

$$\begin{aligned} p &= (\xi - \psi), \quad g = (t - \psi) \\ p &= (\xi - \psi), \quad g = (-t - \psi) \\ p &= (-\xi - \psi), \quad g = (t - \psi) \\ p &= (-\xi - \psi), \quad g = (-t - \psi) \end{aligned}$$

respectively, and denote

$$R = e^{-bp^2} e^{-bg^2}$$

then we have finally

$$\begin{aligned} \omega^2(\psi) = \frac{1}{d^2} & \left\{ \int_{-\psi}^\infty \int_{-\psi}^\infty R u(p+\psi) u(g+\psi) dg dp \right. \\ & - \int_{-\psi}^\infty \int_{-\infty}^{-\psi} R u(p+\psi) u(-\psi-g) dg dp \\ & - \int_{-\infty}^{-\psi} \int_{-\psi}^\infty R u(-\psi-p) u(g+\psi) dg dp \\ & \left. + \int_{-\infty}^{-\psi} \int_{-\infty}^{-\psi} R u(-\psi-p) u(-\psi-g) dg dp \right\} \end{aligned}$$

Restricting u to be an odd function this equation simplifies to

$$w^2(\psi) = \frac{1}{d^2} \int_{-\infty}^{+\infty} \int_{-\infty}^{+\infty} R u(p+\psi) u(g+\psi) dg dp$$

Now, since

$$\|z\|^2 = \int_0^{\infty} z(\psi)^2 d\psi$$

we have

$$\|z\|^2 = \frac{1}{d^2} \int_0^{\infty} d\psi \int_{-\infty}^{\infty} \int_{-\infty}^{\infty} R u(p+\psi) u(g+\psi) dg dp$$

Inverting the order of integration and making use of the Schwartz inequality,

$$\int_0^{\infty} f(p+\psi) f(g+\psi) d\psi \leq \|f\|^2$$

this reduces to

$$\|z\|^2 \leq \|u\|^2 \frac{1}{d^2} \int_{-\infty}^{\infty} \int_{-\infty}^{\infty} R dg dp = \|u\|^2 \int_{-\infty}^{\infty} \int_{-\infty}^{\infty} e^{-bp^2 - bg^2} dg dp$$

which is simply

$$\|z\|^2 \leq \|u\|^2 \frac{\pi}{d^2 b} = \|u\|^2$$

Thus,

$$\|B\| = \sup_{\|u\| \neq 0} \frac{\|Bu\|}{\|u\|} = \sup_{\|u\| \neq 0} \frac{\|z\|}{\|u\|} \leq \frac{\|u\|}{\|u\|} = 1$$

and likewise $\|A\| \leq 1$, which yields

$$\|c\| = \|AB\| < \|A\| \|B\| < 1$$

Therefore, in order for $\lambda < 1/\|c\|$, we must have $\lambda \leq 1$ and, since in our case $\lambda = 1$, the solution is valid everywhere and the series expressed by equation 25 is convergent.

APPENDIX II

The integral

$$E = \int_0^{\infty} \frac{1}{2\sqrt{\pi x}} \operatorname{erf}\left(\sqrt{\frac{1}{\phi}} \frac{\psi}{2}\right) \left\{ \exp(-1/4x)(\psi-\xi)^2 - \exp(-1/4x)(\psi+\xi)^2 \right\} d\xi \quad (\text{II-1})$$

may be evaluated in the following manner. Noting that

$$\operatorname{erf}\left(\sqrt{\frac{1}{\phi}} \frac{\psi}{2}\right) = \int_0^{\infty} \frac{1}{2\sqrt{\pi\phi}} \left\{ \exp(-1/4\phi)(z-\psi)^2 - \exp(-1/4\phi)(z+\psi)^2 \right\} dz \quad (\text{II-2})$$

we may substitute equation II-2 in equation I-1 to get

$$E = \frac{1}{2\sqrt{\pi x}} \int_0^{\infty} \int_0^{\infty} \frac{1}{2\sqrt{\pi\phi}} \left\{ \exp(-(z-p)^2/4\phi) - \exp(-(z+p)^2/4\phi) \right\} dz \left\{ \exp(-(p-\psi)^2/4x) - \exp(-(p+\psi)^2/4x) \right\} dp$$

After carrying out the multiplication, and inverting the order of integration, use of the hyperbolic identity $2 \sinh b = e^x - e^{-x}$ yields

$$E = \frac{1}{\pi\sqrt{x\phi}} \int_0^{\infty} \int_0^{\infty} \exp\left(-\frac{(x+\phi)p^2}{4\phi x} - \frac{xz^2 + \phi\psi^2}{4\phi x}\right) \left(\sinh \frac{p\psi\phi}{2\phi x} \sinh \frac{p x z}{2\phi x} \right) dp dz$$

Making use of the identity

$$\sinh A \sinh B = \cosh(A+B) - \cosh(A-B)$$

we have

$$E = \frac{1}{\pi\sqrt{x\phi}} \int_0^{\infty} \int_0^{\infty} \exp\left(-\frac{(x+\phi)p^2}{4\phi x} - \frac{xz^2 + \phi\psi^2}{4\phi x}\right) \\ \left\{ \cosh\left(\frac{p}{2}\left(\frac{\psi}{x} + \frac{z}{\phi}\right)\right) - \cosh\left(\frac{p}{2}\left(\frac{\psi}{x} - \frac{z}{\phi}\right)\right) \right\} dp dz$$

This expression when integrated¹⁹ and simplified yields

$$E = \frac{1}{2\sqrt{\pi(x+\phi)}} \int_0^{\infty} \left\{ \exp\left(-\frac{(z-\psi)^2}{4(x+\phi)}\right) - \exp\left(-\frac{(z+\psi)^2}{4(x+\phi)}\right) \right\} dz$$

which from equation II-2 reduces to

$$E = \operatorname{erf}\left(\sqrt{\frac{1}{x+\phi}} \frac{\psi}{2}\right)$$

APPENDIX III

The condition $\|AB\| < \|A\| \|B\|$ for the kernels given in equation I-1 may be shown in the following manner. The operators A, B are defined such that

$$\begin{aligned} u(\psi) = A w(\psi) &= z \int_0^{\infty} w(\xi) g_1(\psi, \xi) d\xi \\ &= \int_{-\infty}^{\infty} w(\xi) g_1(\psi, \xi) d\xi \end{aligned}$$

$$B w(\psi) = \int_{-\infty}^{\infty} w(\xi) h_1(\psi, \xi) d\xi,$$

where the kernels are

$$g_1(\psi, \xi) = \frac{1}{2\sqrt{\pi x_m}} \left\{ \exp\left(-(\psi-\xi)^2/4x_m\right) - \exp\left(-(\psi+\xi)^2/4x_m\right) \right\}$$

$$h_1(\psi, \xi) = \frac{1}{2\sqrt{\pi x_s}} \left\{ \exp\left(-(\psi-\xi)^2/4x_s\right) - \exp\left(-(\psi+\xi)^2/4x_s\right) \right\}$$

and

$$w \in L^2$$

$$A, B \in L(L^2, L^2)$$

Now

$$A(Bw)(\psi) = \int_{-\infty}^{\infty} g_1(\psi, z) \int_{-\infty}^{\infty} w(\xi) h_1(z, \xi) d\xi dz$$

and interchange of the order of integration yields

$$A(Bw)(\psi) = \int_{-\infty}^{\infty} w(\xi) \int_{-\infty}^{\infty} g_1(\psi, z) h_1(z, \xi) dz d\xi$$

or

$$A(Bw)(\psi) = \int_{-\infty}^{\infty} w(\xi) H(\psi, \xi) d\xi,$$

where $H(\psi, \xi)$ is defined as the inner integral, and

$$H \in \mathbb{R}^2 [R \times R] \quad . \quad (\text{See Reference 20, p. 156})$$

Thus

$$\|AB\|^2 = \int_{-\infty}^{\infty} \int_{-\infty}^{\infty} |H(\psi, \xi)|^2 d\psi d\xi = \|H\|^2$$

and making use of the Cauchy inequality it follows

$$\begin{aligned} |H(\psi, \xi)|^2 &= \left| \int_{-\infty}^{\infty} g_1(\psi, z) h_1(z, \xi) dz \right|^2 \\ &\leq \int_{-\infty}^{\infty} |g_1(\psi, z)|^2 dz \int_{-\infty}^{\infty} |h_1(z, \xi)|^2 dz \end{aligned}$$

$$\|AB\|^2 \leq \|A\|^2 \|B\|^2$$

If we assume ψ and ξ are the nonequal constants $\psi_0, \xi_0 < \infty$ in the integrals above, we can replace g_1 and h_1 with g_2 and h_2 , where

$$g_2(z) = g_1(\psi_0, z)$$

$$h_2(z) = h_1(z, \xi_0)$$

This assumption yields

$$|H(\psi, \xi)|^2 \leq \int_{-\infty}^{\infty} |g_2(z)|^2 dz \int_{-\infty}^{\infty} |h_2(z)|^2 dz,$$

where the equality sign applies if and only if g_2 and h_2 are dependent.

Now since we have

$$g_2(z) = \frac{1}{2\sqrt{\pi X_m}} \left\{ \exp\left(-\frac{(\psi_0 - z)^2}{4X_m}\right) - \exp\left(-\frac{(\psi_0 + z)^2}{4X_m}\right) \right\}$$

$$h_2(z) = \frac{1}{2\sqrt{\pi X_s}} \left\{ \exp\left(-\frac{(\xi_0 - z)^2}{4X_s}\right) - \exp\left(-\frac{(\xi_0 + z)^2}{4X_s}\right) \right\}$$

g_2 and h_2 are certainly independent and $\|AB\| < \|A\| \|B\|$ at the point ψ_0, ξ_0 . Since it is easily seen that $\|AB\| < \|A\| \|B\|$ for any neighborhood of ψ_0 and ξ_0 , we state that $\|AB\| < \|A\| \|B\|$ in all space for the kernels considered.

REFERENCES

1. Prandtl, L., "Uber Flussigkeitsbewegung bei sehr kleiner Reibung," Proc. III International Math. Congr., Heidelberg 1904. Reprinted in NACA Tech. Memo No. 452, 1928.
2. Mills, R.D., "On the Closed Motion of a Fluid in a Square Cavity," J. Roy. Aero. Soc. 69, p. 116, 1965.
3. Ringleb, F.O., "Discussion of Problems Associated with Standing Vortices and Their Applications," Paper presented at ASME Fluids Engineering Division Conference, Philadelphia, Pa., May 18-20, 1964.
4. Thom, A. and Apelt, C., "The Pressure on a Two-Dimensional Static Hole at Low Reynolds Number," ARC R&M 3090, 1957.
5. Batchelor, G.K., "On Steady Laminar Flow with Closed Streamlines and Large Reynolds Numbers," J. Fluid Mech. 1, p. 177, 1956.
6. Wood, W.W., "Boundary Layers Whose Streamlines are Closed," J. Fluid Mech. 2, p. 77, 1957.
7. Roshko, A., "Some Measurements of Flow in a Rectangular Cutout," NACA TN 3488, 1955.
8. Weiss, R.F. and Florsheim, B.H., "Flow in a Cavity at Low Reynolds Number," Physics of Fluids, 8, p. 1631, 1965.
9. Mills, R.D., "Numerical Solutions of the Viscous Flow Equations for a Case of Closed Flows," J. Roy. Aero. Soc., 69, p. 714, 1965.
10. Burggraf, O.R., "Analytical and Numerical Studies of the Structure of Steady Separated Flows," J. Fluid Mech. 24, p. 113, 1966.
11. Pan, F. and Acrivos, A., "Steady Flow in Rectangular Cavities," J. Fluid Mech., 28, p. 643, 1967.
12. Squire, H.B., "Note on the Motion Inside a Region of Recirculation (Cavity Flow)," J. Roy. Aero. Soc., 60, p. 203, 1956.
13. Lewis, J.A. and Carrier, G.F., "Some Remarks on the Flat Plate Boundary Layer," Quart. Appl. Math., 7, p. 228, 1962.
14. Sparrow, E.M. and Lin, S.H., "Flow Development in the Hydrodynamic Entrance Region of Tubes and Ducts," Physics of Fluids, 7, p. 338, 1964.
15. Schlichting, H., "Boundary Layer Theory," Chapter 8, McGraw Hill, New York, 1955.
16. Stakgold, I., "Boundary Value Problems of Mathematical Physics, Vol. 1," Chapter 3, MacMillan, New York, 1967.

17. Howarth, L., "On the Solution of the Laminar Boundary Layer Equations," Proc. Roy. Soc., London, A, 164, p. 547, 1938.
18. Friedman, B., "Principles and Techniques of Applied Mathematics," Wiley, New York, 1956.
19. Gradshteyn, I.S. and Ryzhik, I.M., "Table of Integrals, Series and Products," p. 357, Academic, New York, 1965.
20. Riesz, F., and Sz-Nagy, B., "Functional Analysis," Ungar, New York, 1955.

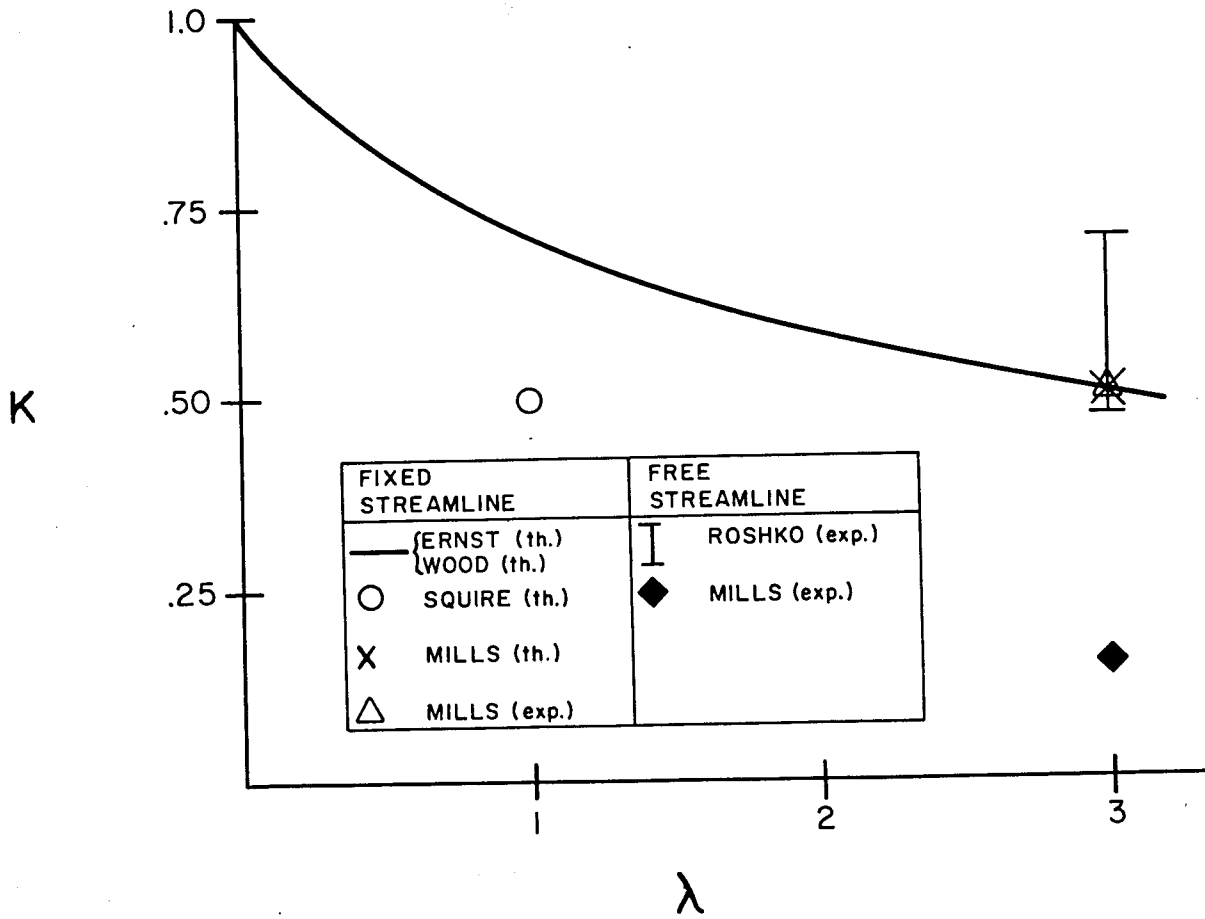


Fig. 3. Core Velocity Ratio Versus Wall Length Ratio

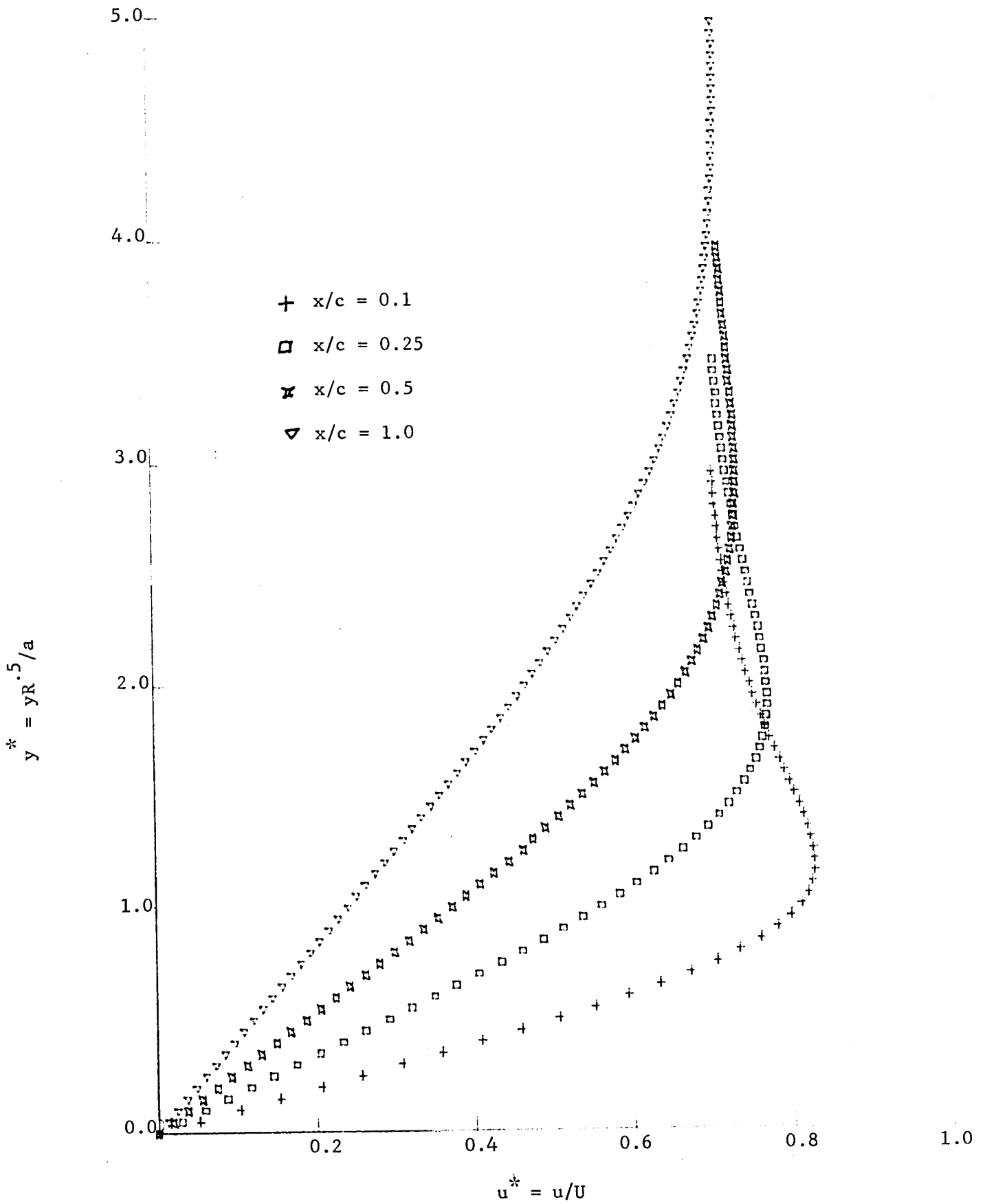


Fig. 4a.

Qualitative Boundary Layer Velocity Profiles on Stationary Wall
 for $\lambda = 1$ Case with $k_{m_0} = k_{s_0} = 2$.

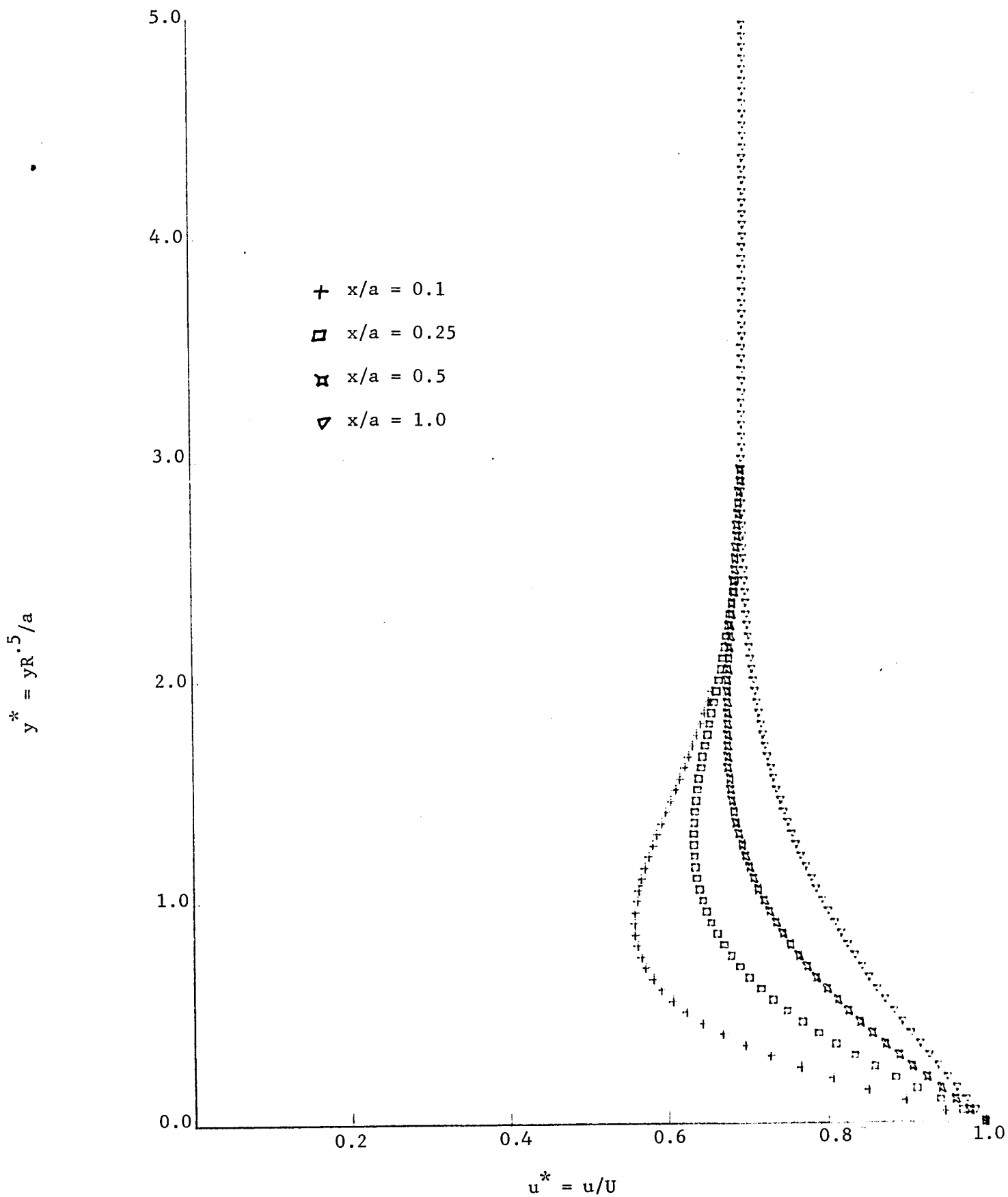


Fig. 4b.

Qualitative Boundary Layer Velocity Profiles on Moving Wall
 for $\lambda = 1$ Case with $k_{m_0} = k_{s_0} = 2$.

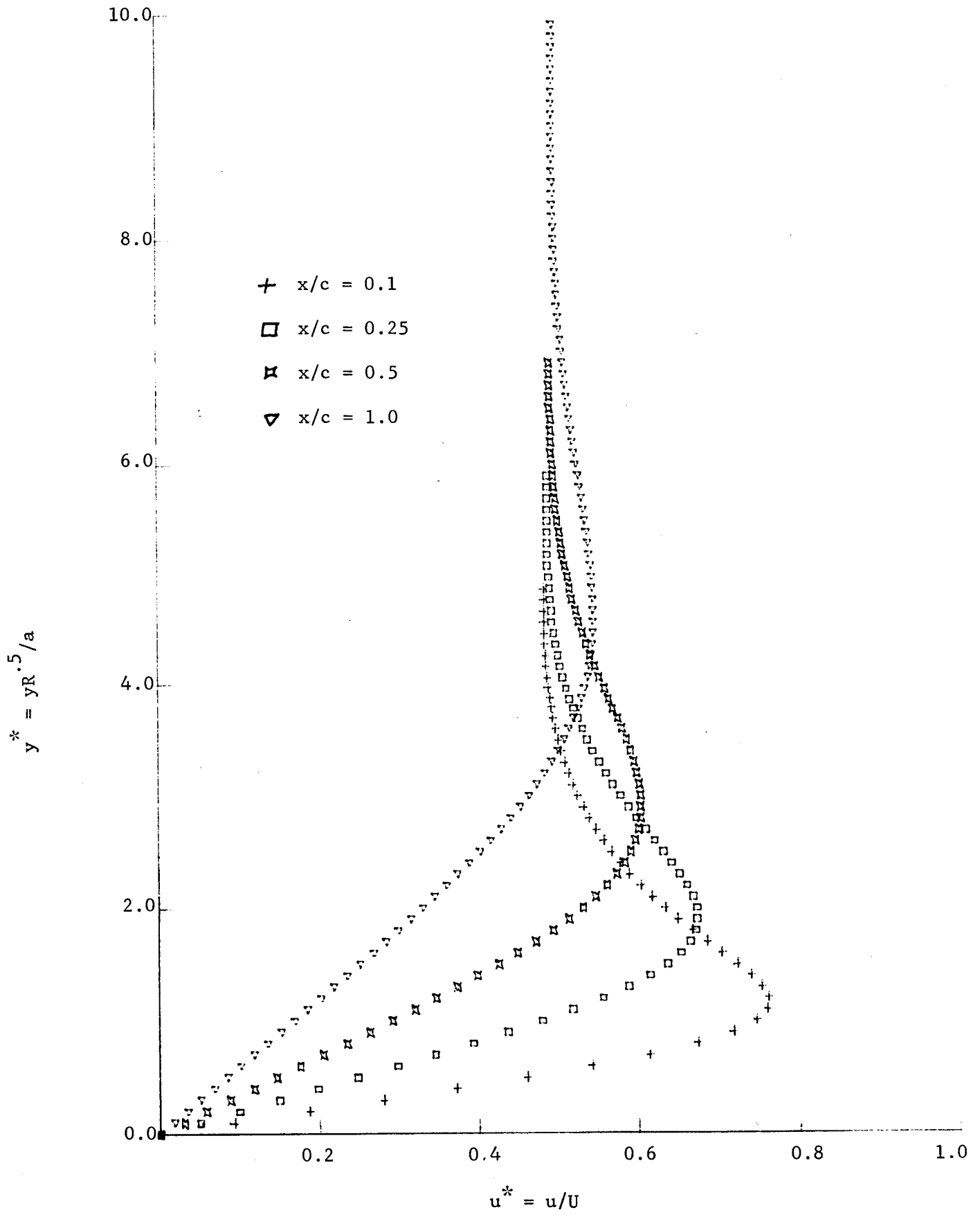


Fig. 5a.

Qualitative Boundary Layer Velocity Profiles on Stationary Wall
 for $\lambda = 3$ Case with $k_{m_0} = k_{s_0} = 2$.

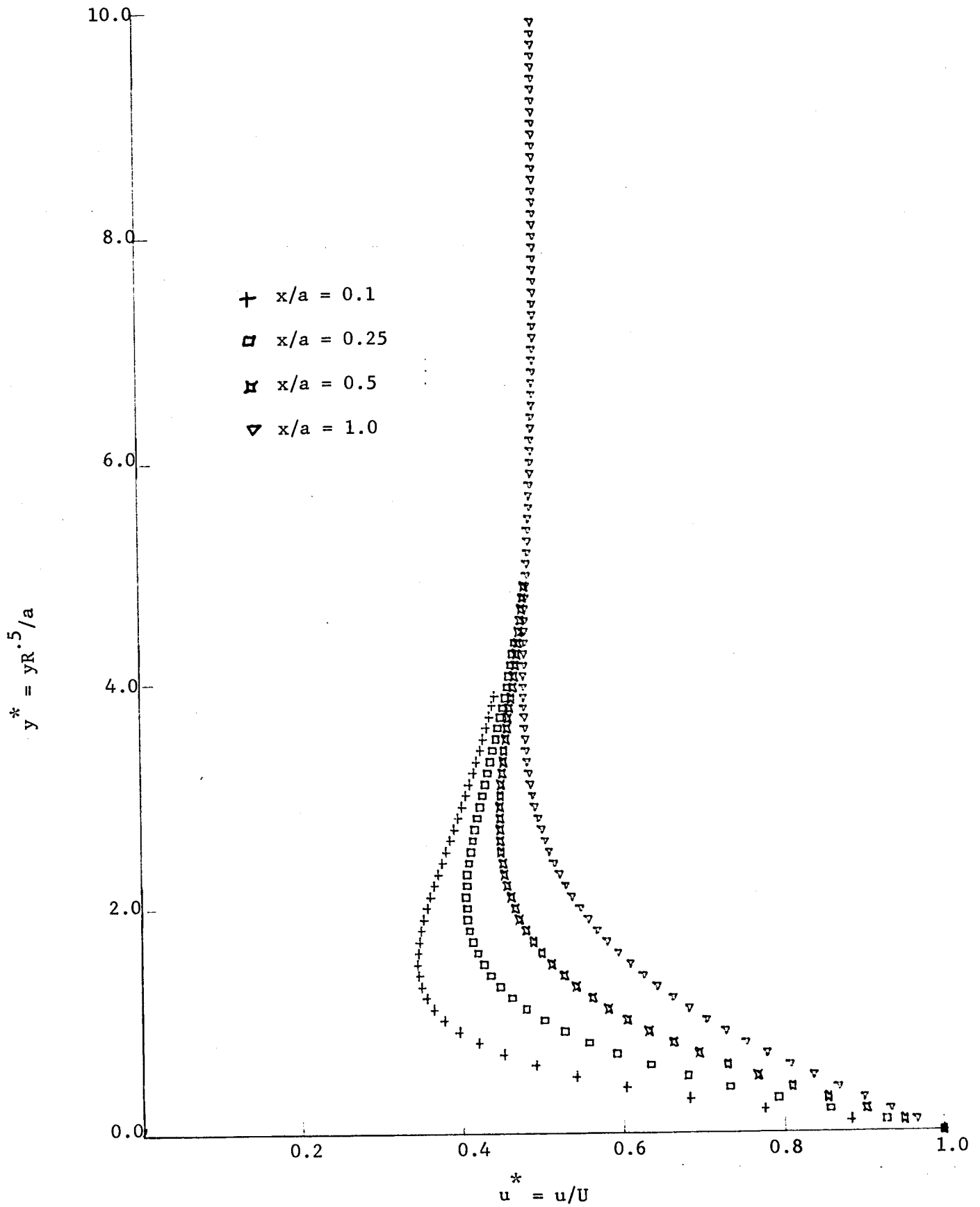


Fig. 5b.

Qualitative Boundary Layer Velocity Profiles on Moving Wall
 for $\lambda = 3$ Case with $k_{m_0} = k_{s_0} = 2$.